Limit of Spatial Resolution in FDG-PET due to Annihilation Photon Non-Collinearity

Chapter · January 2007

DOI: 10.1007/978-3-540-36841-0_411

8 authors, including:

Kengo Shibuya
The University of Tokyo
122 PUBLICATIONS **928** CITATIONS

SEE PROFILE

Limit of Spatial Resolution in FDG-PET due to Annihilation Photon Non-Collinearity

K. Shibuya[1], E. Yoshida[1], F. Nishikido[1], T. Suzuki[2], T. Tsuda[1], N. Inadama[1], T. Yamaya[1] and H. Murayama[1]

[1] Molecular Imaging Center, National Institute of Radiological Sciences, Chiba 263-8555, Japan
[2] Research Center for Radiation Emergency Medicine, National Institute of Radiological Sciences, Chiba 263-8555, Japan

Abstract— **We provide a new viewpoint for a fundamental but little investigated problem in positron emission tomography (PET): non-collinearity of annihilation radiation from the human body. The cause of the angular deviation from 180 deg is described as well as how to evaluate it under a spatially distributed radiation source and a limited acquisition time. An elegant conversion from the photopeak spectrum into the angular distribution is done based on the conservation laws of momentum and energy to avoid problems in the direct measurement. A healthy volunteer study using ^{18}FDG and a Ge semiconductor detector reveals the distribution as a Gaussian function with the FWHM of 0.54 deg. Finally, we calculate the physical limit of ^{18}FDG-PET spatial resolution.**

Keywords— **angular deviation, in vivo study, spatial resolution, Doppler Effect, Ge semiconductor detector**

I. Introduction

PET is receiving much attention from the researchers in the field of molecular imaging [1, 2]. The electron-positron pair annihilation (EPA) provides the position of a target molecule by two radiations emitted simultaneously in opposite directions. The molecular most probably exists on the line of response (LOR) between the two activated detectors. To improve the spatial resolution, many investigators have been developed pixelized detectors [3].

There are two physical limits for the spatial resolution: positron range and non-collinearity of the EPA radiation (EPAR). First, the position of the positron emission and the EPA are not the same because of initial emission energy. According to Levin and Hoffman [4], full-width at half-maximum (FWHM) of the positron range in water is 0.10 mm for ^{18}F and 0.50 mm for ^{15}O. Second, the flights of the two annihilation radiations are not exactly collinear. The slight angle deviation from 180° causes a departure of the annihilation point to the LOR.

The aim of this study is a quantitative determination of the angle distribution of the EPAR from the human body. In 1965, Colombino *et al.* [5] measured the distribution for pure water at 4°C and the result of about 0.47° for FWHM is still often referred to [4, 6, 7]. However, the distribution changes considerably with some chemical and physical conditions such as ionic concentrations and temperature [5, 8-10].

No data on the angular distribution for the human body are available because of the measurement difficulty. Generally, a direct measurement is performed using two position sensitive detectors such as Anger cameras. A triangle, formed by the two activated detectors and the one source position, is determined in every coincidental event. The detectors are located several meters distance to enhance the angular resolution at the cost of the counting rate [9, 11]. However, this method supposes a point source at a known position and a sufficient acquisition time often longer than a week. In the case of a human PET study, however, only a limited amount of short-lived nuclides is injected and spatially distributed in the body.

II. Theory

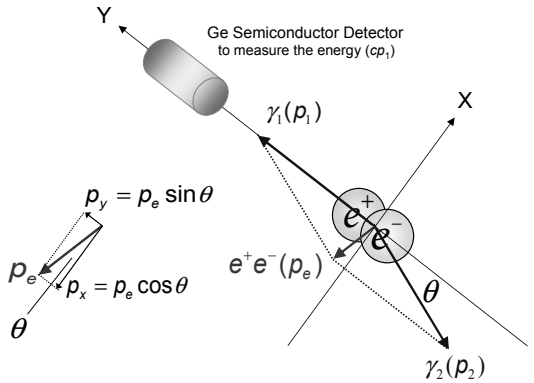

Fig. 1 A coordinate system to formulate the conservation laws of momentum and energy before and after the annihilation.

In this paper, we solve the problem of how to determine the angular distribution of the EPAR with a distributed source and a limited time. We measure another physical quantity which is converted into the angle. Figure 1 shows a laboratory system to formulate the physical conservation laws. The EPA takes place at the origin, and one of the two radiation photons is emitted along with the y-axis, and the other is emitted at an angle of θ in the minus y-direction. The x-axis is defined perpendicular to the y-axis. The momentum vector of the former radiation is defined as p_1, and that of the latter one is p_2. p_e is the momentum vector of the mass center of the electron-positron (*e*-*p*) pair before the annihilation.

We can see the law of conservation of momentum in Fig. 1 displayed by a parallelogram formed by the above three vectors. The equations are

$$p_x \equiv p_e \cos\theta = p_2 \sin\theta \quad (1)$$

in the x-direction and

$$p_y \equiv p_e \sin\theta = p_1 - p_2 \cos\theta \quad (2)$$

in the y-direction. The left side and the middle term of each equation represent the *e-p* momentum in each direction, and the right side is that of the two photons after the annihilation. The law of conservation of energy is formulated using the Einstein's mass-energy equation, *i.e.*, $E = \sqrt{M^2c^4 + p^2c^2}$, as

$$2mc^2 = cp_1 + cp_2, \quad (3)$$

where E is the energy, M is the mass, p is the momentum, and c is the speed of light *in vacuo*. The left side is the rest mass energy of the *e-p* pair (p=0), where the mass of each electron is m. Their relatively small kinetic energy is ignored. The right side is the energy of the two radiations (M=0).

Since the same numbers of equations and independent variables (p_1, p_2, θ) are obtained, a determination of one physical quantity fixes the other two quantities. In this study, we measure the energy of the former radiation (cp_1), and then, momentum of the radiation (p_1), energy and momentum of the latter radiation (cp_2, p_2), and the angle (θ) were fixed at once. No necessity for any coincidental measurements significantly reduces the acquisition time.

The energy of each EPAR is obtained by solving Eqs. (2) and (3) simultaneously as

$$\begin{cases} cp_1 = \dfrac{2mc^2 + cp_y}{1+\cos\theta} \sim mc^2 + \dfrac{cp_y}{2} \\ cp_2 = \dfrac{2mc^2 - cp_y}{1+\cos\theta} \sim mc^2 - \dfrac{cp_y}{2} \end{cases} \quad (4)$$

with the small angle approximation of $\cos\theta \sim 1$. We obtain a different radiation energy than the rest mass energy of one electron, and the deviation is proportional to $|p_y|$. In other words, the source of the high-energy light wave is moving toward/away from the observer, so a shorter/longer photonic wavelength than 511 keV is measured: this is the Doppler Effect due to the wave nature of the radiation photon [12].

The angular deviation is obtained when the p_2 in Eq. (4) is substituted for that in Eq. (1) as

$$p_x = p_2 \sin\theta \sim mc\theta \quad (5)$$

with the approximation of $\sin\theta \sim \theta$ and the assumption of $mc \gg p_y$. The angular deviation is proportional to $|p_x|$. In brief, the x-component of the *e-p* momentum is conserved as the angular deviation from 180°, and the y-component is conserved as the energy deviation from 511 keV.

Here, p_x and p_y are considered to be statically the same because the electron momentum distribution must be isotropic in the human body. With this natural premise, the relationship between the energy deviation and the angular deviation of the EPAR is obtained from Eqs. (4) and (5) as

$$2\langle \Delta E \rangle / mc^2 = \pm \langle \theta \rangle \quad (6)$$

where $\langle \Delta E \rangle$ is the distribution of the energy deviation from 511 keV, and $\langle \theta \rangle$ is the distribution of the angular deviation from 180°. The two distributions can be converted into each other.

III. Experimental

For a precise measurement of $\langle \Delta E \rangle$, a Ge detector (GEM-25, ORTEC) is employed. To calibrate the detector, six kinds of radioactive nuclides, ^{241}Am, ^{133}Ba, ^{57}Co, ^{22}Na (positron emitter), ^{137}Cs, ^{54}Mn, and ^{88}Y, sealed in each plastic container are measured simultaneously. A pulse-height analyzer attached to the detector has a 13-bit analog digital converter, and each channel occupies 0.11 keV in this paper. The detector is kept 2.0 m from the scanning bed so that the dead-time rate does not exceed 5%.

One hundred megabecquerels (2.8 mCi) of 2-[^{18}F]-fluoro-2-deoxy-D-glucose (^{18}FDG) [2, 13] are injected into a healthy volunteer (22-years old male) to evaluate a brain PET scanner named jPET-D4 [14, 15]. After a 140-min rest, a 40-min continuous acquisition is done.

IV. Results and Discussion

Figure 2 (a) shows the spectrum of the six nuclides. Photopeaks of higher energy tend to have a broader form except for the EPAR peak at 511 keV. The relationship between the energy and the photopeak FWHM is plotted in Fig. 2 (b), including the result of the *in vivo* ^{18}FDG. Theoretically, the photopeak FWHM is proportional to the square root of the energy because the number of electron-hole pairs excited in the detector is subject to a Poisson distribution. Eight photopeaks due to the five nuclides are well fitted by the parabola, while the photopeaks due to the EPAR are clearly broader because of the Doppler Effect. The greater Doppler Effect can be attributed to the mass of the *e-p* pairs which is much smaller than that of a nucleus.

Figure 3 shows the spectrum of the EPAR from the *in vivo* ^{18}FDG and its magnified photopeak. The photopeak count defined by the energy between 504.0 and 518.0 keV is 1.7×10^5. The photopeak form is well fitted by a Gaussian function, and the FWHM is 2.68 keV. However, a shape different from the Gaussian is observed around vertex and occupies 0.6% of the photopeak. This minor component is attributed to a positronium, a short-lived hydrogen-like "atom" composed of an electron and a positron, whose elec-

tron has lost the original orbital momentum when captured by the positron. Because the EPAR from pure water typically exhibits the positronium component of around 10% [9], the chemical and physical conditions in the human body seems not to be the same as in pure water for a positron and/or a positronium.

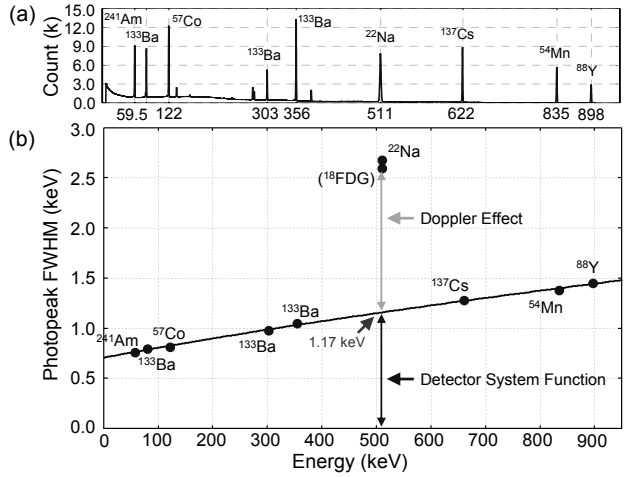

Fig.2 (a) The spectrum of the six radioactive nuclides, and (b) the relation ship between the radiation energy and the photopeak FWHM.

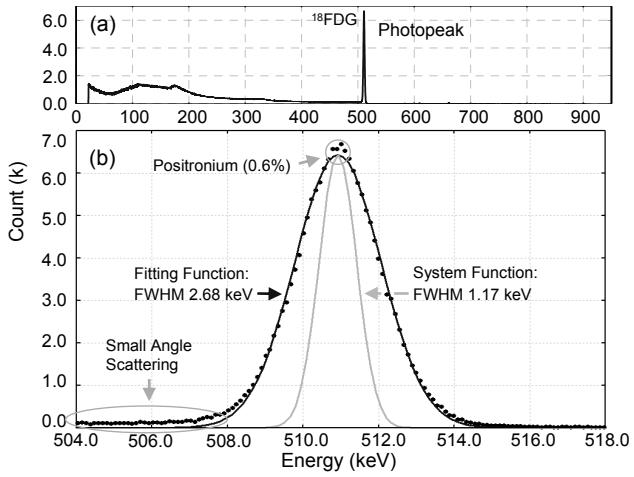

Fig.3 (a) Spectrum of *in vivo* ^{18}FDG and (b) the magnified photopeak fitted by a Gaussian function (black line). The gray line is the estimated system function of the Ge semiconductor detector at 511 keV.

Generally, the form of a gamma-ray photopeak, $F(E)$, is explained by the convolution of a delta function of the gamma-ray energy distribution and a system function of the detector, $H(E)$, as

$$F(E) = H(E) \otimes \delta(E) \qquad (7)$$

where $\otimes$ is a convolution operator. On the other hand, the form of the EPAR photopeak is described with an additional convolution as

$$F(E) = H(E) \otimes D(E) \otimes \delta(E) \qquad (8)$$

where $D(E)$ is the "system function" of the Doppler Effect. Without the Doppler Effect, the FWHM should have been 1.17 keV at 511 keV as shown in Fig. 2 (b), while the measured one was 2.68 keV as shown in Fig. 3 (b). The $D(E)$ is obtained when $F(E)$ is deconvoluted by $H(E)$ to remove the detector's system function. Since both $F(E)$ and $H(E)$ are well described by Gaussian functions, $D(E)$ can also be described by a Gaussian function, and the FWHM is calculated from the FWHMs of $D(E)$ and $H(E)$ as $\sqrt{2.68^2 - 1.17^2} \sim 2.4$ keV.

The obtained distribution of ΔE can be converted into the distribution of θ by using Eq. (4). As the result, the angular distribution of EPAR from ^{18}FDG in the human body is determined to be a Gaussian distribution with the FWHM of 9.4 mrad=0.54°. The value is about 15% larger than that have obtained for pure water [5].

From this result, we can calculate the physical limit of the PET spatial resolution. A forward projection of the ideal line source placed on the center axis is described as

$$P(x) = P_r(x) \otimes P_a(x) \otimes P_d(x) \otimes \delta(x) \qquad (9)$$

where $P_r(x)$ is line spread function due to the positron range, $P_a(x)$ is that due to the angular deviation, $P_d(x)$ is that due to the detectors and other electronics, and $\delta(x)$ is a delta function representing the distribution of activity of the ideal line source. Therefore, $P_r(x) \otimes P_a(x)$ gives the physical limit of PET spatial resolution.

The distance between the true LOR and the false LOR due to the angular deviation of θ is written as

$$\Delta t = R \sin(\theta/2) \qquad (10)$$

where R is the radius of the detector ring. This equation gives the FWHM of the Gaussian function of $P_a(x)$. Therefore, we obtain

$$P_a(x) = \frac{1}{\sqrt{2\pi}\sigma} \exp\left(-x^2 \Big/ 2\sigma^2\right) \qquad (11)$$

with the standard deviation σ as

$$\sigma(R) = \frac{R \sin(0.54^\circ/2)}{2.35} = 2.01 \times 10^{-3} R \ . \qquad (12)$$

According to Derenzo [16], the positron range distribution can be written by an even function of dual-exponential as

$$P_r(x) = \begin{cases} Ce^{-k_1 x} + (1-C)e^{-k_2 x}, x \geq 0 \\ Ce^{k_1 x} + (1-C)e^{k_2 x}, x < 0 \end{cases} \qquad (13)$$

with three parameters of C, k_1 and k_2. These values were determined experimentally by Derenzo [16], and computationally by Levin and Hoffman [4] and by Palmer *et al.* [7]. Their results for ^{18}F in water are shown in Fig. 4 (a) with the

plots for $x \le 0$. Regarding the FWHM, the results by Derenzo (dashed line) and by Levin and Hoffman (solid line) are in good agreement. On the other hand, for the full width at tenth maximum (FWTM), the results by Levin and Hoffman and by Palmer *et al*. (dotted line) are in fair agreement. We employ the results by Levin and Hoffman to calculate the limit of PET spatial resolution.

The larger the detector ring radius, the greater spatial blurring occurs because of the non-collinearity. Figure 4 (b) shows the convolution results of $P_r(x) \otimes P_a(x)$ with $P_r(x)$ for ^{18}F and $P_a(x)$ for the R of 5.0, 20 and 40 cm. The FWHM of the line spread function is 0.5 mm for R=5 cm, *e.g.*, small animal PET, 1.2 mm for R=20 cm, *e.g.*, human brain PET, and 2.1 mm for R=40 cm, *e.g.*, human wholebody PET. These values give the physical limits of PET spatial resolution with the ideal position sensitive radiation detectors: $P_d(x) \equiv \delta(x)$.

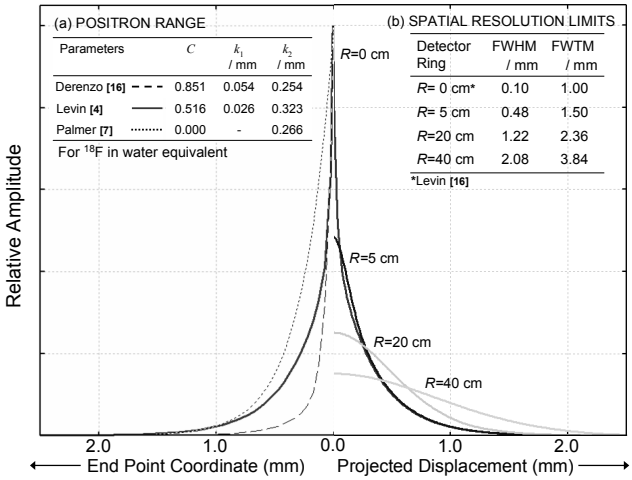

Fig. 4 (a) Positron range for ^{18}Fe reported by three groups. The inset table on the left shows their parameters. (b) The convolution results of the positron range by Levin and Hoffman and the angular deviation function determined in this paper. The inset table on the right shows the FWHMs and FWTMs.

V. Conclusions

The non-collinearity of electron-positron annihilation radiation from *in vivo* ^{18}FDG was evaluated for the first time by the conversion from the photopeak spectrum into the angular deviation. The distribution was well described by a Gaussian function centered at 0˚ with the FWHM of 0.54˚, which was about 15% larger than the value for pure water. Therefore, the chemical and physical conditions in the human body are not the same as those in pure water for a positron and/or positronium. Because the present results were obtained under the same conditions as for clinical ^{18}FDG-PET scans, they may be used reliably for simulations, system designs, image reconstructions, *etc*. For example, the limit of PET spatial resolution are calculated to be 0.5 mm for a 10-cm diameter scanner, 1.2 mm for a 40-cm diameter scanner, and 2.1 mm for an 80-cm diameter scanner.

Acknowledgments

We would like to thank M. Koshimizu with Tohoku Univ. and M. Yuuki with Tokyo Nuclear Services Co. for technical advice on using the Ge detector. K. S is supported by a post-doctoral research fellowship from JSPS.

References

1. Rudin M, Weissleder R (2003) Molecular imaging in drug discovery… Nature Rev Drug Discov 2: 123-131
2. Gambhir SS (2002) Molecular imaging of cancer with positron emission tomography. Nature Rev Cancer 2: 683-693
3. Budinger TF (1998) PET instrumentation: What are the limits? Semin Nucl Med 28: 247-267
4. Levin CS, Hoffman EJ (1999) Calculation of positron range and its effect… J Nucl Med 44: 781-799
5. Colombino P, Fiscella B, Trossi L (1965) Study of positronium in water and ice… IL NUOVO CIMENT 38: 707-723
6. Derenzo SE, Budinger TF (1977) Resolution limit for positron-imaging devices. J Nucl Med 18: 491-492
7. Palmer MR, Zhu XP et al. (2005) Modeling and simulation of positron range effects… IEEE Trans Nucl Sci 52: 1391-1395
8. DeZafra RL (1959) Effect of impurities of angular correlation of positron annihilation radiation. Phys Rev 113: 1547-1555
9. Trumpy G (1960) Positron annihilation in aqueous solutions. Phys Rev 118: 668-674
10. DeZafra RL, Joyner WT (1958) Temperature effect on positron annihilation in condensed matter. Phys Rev 112: 19-29
11. Fujiwara K, Sueoka O (1966) A precise measurement of the angular correlation of annihilation radiation in copper single crystals. J Phys Soc Jpn 21: 1947-1955
12. Hotz HP et al. (1968) Measurement of positron annihilation line shapes with a Ge(Li) detector. Phys Rev 170: 351-355
13. Gambhir SS et al. (2001) A tabulated summary of the FDG PET literature. J Nucl Med 42: 1S-93S
14. Yamaya T et al. (2005) Transaxial system model for jPET-D4 image reconstruction. Phys Med Biol 50: 5339-5355
15. Orita N et al. (2005) Three-dimensional array of scintillation crystals with proper reflector… IEEE Trans Nucl Sci 52: 8-14
16. Derenzo SE (1986) Mathematical removal of positron range blurring… IEEE Trans Nucl Sci 33: 565-569

Address of the corresponding author:

Author: Dr. Kengo Shibuya
Institute: Department of Biophysics, Molecular Imaging Center, National Institute of Radiological Sciences
Street: Anagawa 4-9-1
City: Inage, Chiba 263-8555
Country: Japan
Email: shibuken@nirs.go.jp